Magnetic and structural properties of an octanuclear Cu(II) $S=1/2$ mesoscopic ring: Susceptibility and NMR measurements

A. Lascialfari
Department of Physics ''A. Volta'' and Unita INFM, University of Pavia, Via Bassi 6, I-27100 Pavia, Italy

Z. H. Jang
Ames Laboratory and Department of Physics and Astronomy, Iowa State University, Ames, Iowa 50011

F. Borsa
Department of Physics ''A. Volta'' and Unita INFM, University of Pavia, Via Bassi 6, I-27100 Pavia, Italy and Ames Laboratory and Department of Physics and Astronomy, Iowa State University, Ames, Iowa 50011

D. Gatteschi
Department of Chemistry, University of Florence, Via Maragliano 77, I-50144 Florence, Italy

A. Cornia
Department of Chemistry, University of Modena, Via Campi 183, I-41100 Modena, Italy

D. Rovai and A. Caneschi
Department of Chemistry, University of Florence, Via Maragliano 77, I-50144 Florence, Italy

P. Carretta
Department of Physics ''A. Volta'' and Unita INFM, University of Pavia, Via Bassi 6, I-27100 Pavia, Italy
(Received 6 August 1999)

Magnetic susceptibility, ^{1}H NMR and ^{63}Cu NMR-NQR experiments on two slightly different species of the molecular $S=1/2$ antiferromagnetic (AF) ring Cu8, $[Cu_8(dmpz)_8(OH)_8]\cdot 2C_5H_5N$ (Cu8P) and $[Cu_8(dmpz)_8(OH)_8]\cdot 2C_5H_5NO_2$ (Cu8N), are presented. The magnetic energy levels are calculated exactly for an isotropic Heisenberg model Hamiltonian in zero magnetic field. From the magnetic susceptibility measurements we estimate the AF exchange coupling constant $J\sim 1000$ K and the resulting gap $\Delta\sim 500$ K between the $S_T=0$ ground state and the $S_T=1$ first excited state. The ^{63,65}Cu NQR spectra indicate the presence of four crystallographically inequivalent copper nuclei in each ring. From the combination of the ^{63}Cu NQR spectra and of the ^{63}Cu NMR spectra at high magnetic field, we estimate the quadrupole coupling constant υ_Q of each site and the average asymmetry parameter η of the electric-field gradient tensor. The nuclear spin-lattice relaxation rate (NSLR) decreases exponentially on decreasing temperature for all nuclei investigated. The gap parameter extracted from ^{63}Cu NQR-NSLR is the same as for the susceptibility while a smaller value is obtained from the ^{63}Cu NMR-NSLR in an external magnetic field of 8.2 T.

I. INTRODUCTION

Recently, a great effort was made by molecular chemistry in the building up of metal-ion based magnetic mesoscopic clusters with a controlled number of magnetic ions and with exchange coupling constant of different sign and different magnitude.[1] Among these systems the high-symmetry ones, the so-called magnetic molecular rings, are particularly suitable to investigate the link between classical and quantum behavior of low-dimensional compounds. If the number of spins in the ring can be increased in a controlled way the systems are an ideal ''laboratory'' to explore the bridge between microscopic magnetism and collective effects in macroscopic structures. Due to the finite size, these rings have well-defined magnetic energy levels and, in the simplest cases, the eigenvalues and the eigenfunctions can be calculated exactly starting from the appropriate model Hamiltonian.[2] These calculations have remained an academic exercise until now, when real systems are available and allow for a comparison between experiments and exact theories.

Rings with different number of Fe(III) $S=5/2$,[3–5] Cu(II) $S=1/2$,[6,7] V(IV) $S=1/2$,[8] Mn(III) $S=2$ (Ref. 9) ions and different exchange coupling constants are available. The comparison between rings with different metal ions is very useful because some ions (for example Fe(III), $S=5/2$) have a high spin value, which can be modeled as a classical vector to be contrasted with the quantum $S=1/2$ of ions like Cu(II). Moreover, rings with the same metal ion but different crystallographic or magnetic structure have different ground states depending on the bridges between atoms, which lead to different magnetic couplings.[6,7,10]

In this paper we focus on two octanuclear Cu(II) $S=1/2$ rings, $[Cu_8(dmpz)_8(OH)_8]\cdot 2C_6H_5N$ (in short Cu8P) and $[Cu_8(dmpz)_6(OH)_8]\cdot 2C_6H_5NO_2$ (in short Cu8N), in which Cu-Cu antiferromagnetic superexchange coupling leads to a

total spin $S_T=0$ ground state well separated from the first $S_T=1$ excited state. These two Cu8 rings differ only for the crystallization solvent and thus have almost identical magnetic and structural properties. However, both systems were investigated here since they seem to have a different amount of defects, whereby the Cu8N compound has a lower content of defects than that of Cu8P as will be specified later on.

The ^{63,65}Cu NQR signal in the present Cu8 rings was detected in the same frequency range as the ^{63,65}Cu NQR in copper-oxide High-T_c superconductors, spin chains and ladders.[11] The presence of four structurally nonequivalent Cu ions in the ring is confirmed by the presence of four different ^{63}Cu NQR signals. Below room temperature the magnetic properties and the spin dynamics are dominated by the very large energy gap between the singlet ground state ($S=0$) and the first excited triplet state ($S=1$). The measurements of magnetic susceptibility and of nuclear spin-lattice relaxation rate give complementary and consistent information about the value of the magnetic exchange coupling J and of the singlet-triplet energy gap Δ.

In Sec. II we present the experimental methods and the details of the data analysis. In Secs. III, IV, and V we present and analyze the experimental data of susceptibility, static NMR-NQR and spin-lattice relaxation, respectively, while in Sec. VI we compare the different results and give some conclusive remarks.

II. EXPERIMENTAL DETAILS

A. Samples

Polycrystalline samples of $[Cu_8(dmpz)_8(OH)_8]\cdot 2py$ (Cu8P) and $[Cu_8(dmpz)_8(OH)_8]\cdot 2C_6H_5NO_2$ (Cu8N) were synthesized from the polymeric precursor $[Cu(dmpz)]_n$ (where dmpz is the 3,5-dimethylpyrazolate, $C_6H_2N_2$), which was prepared from $[Cu(CH_2CN)_4]BF_4$ and 3,5-dimethylpyrazole as described previously.[12] Cu8P was synthesized according to the procedures in the literature.[13] The nominal composition of $[Cu_8(dmpz)_8(OH)_8]\cdot 2C_5H_5N$ (i.e,. $C_{56}H_{74}Cu_8N_{18}O_8$), would yield for the content of the different elements: C, 38.41%; H, 4.74%; N, 16.13%. The actual content found experimentally for the synthesized compound is: C, 37.90%; H, 4.54%; N, 15.77%. A slightly modified synthetic procedure was used for Cu8N. 6 g of $[Cu(dmpz)]_n$ were suspended in 100 mL of nitrobenzene and the mixture was stirred and heated to reflux for about two days to give a dark green-blue solution. The latter was filtered and left in slow evaporation for a few days, yielding dark blue crystals, which were air-dried and analyzed. The nominal composition for $[Cu_8(dmpz)_8(OH)_8]\cdot 2C_6H_5NO_2$ (i.e., $C_{52}H_{74}Cu_6N_{18}O_{12}$) gives content: C, 37.81%; H, 4.51%; N, 15.26%. For the synthesized compound it was found experimentally: C, 37.88%; H, 4.48%; N, 15.28%. One crystal was checked by x-ray diffraction confirming the unit-cell parameters previously reported for Cu8N:[6] $a=10.233(5)$ Å, $b=27.225(6)$ Å, $c=14.524(5)$ Å, $\beta=98.44(3)°$.

B. Magnetic susceptibility

The magnetic susceptibility data for Cu8N and Cu8P were obtained with a Métronique Ingéniérie MS03 superconducting-quantum interference device (SQUID) Magnetometer in the temperature range 2–260 K, as $\chi=$M/H for $H=1000$ Oe. Isothermal M vs H curves (not reported here) were measured in the Ames Lab by J. E. Ostenson with a Quantum Design MPMS5 SQUID Magnetometer in the temperature range 5–300 K. The magnetization measurements were used to extract the contribution of the paramagnetic defects, which dominate the magnetic response at $T<100$ K due to the very small intrinsic susceptibility of the sample at low temperature. The raw data were corrected for the sample-holder contribution and converted to the mole by using molecular weights 1651.6 and 1563.6, for Cu8N and Cu8P, respectively. Before analyzing the experimental data we have also subtracted from the raw data the contribution due to molecular diamagnetism, estimated from Pascal's constants.[14] The total diamagnetic contribution is found to be $-718\cdot 10^{-6}$ and $-677\cdot 10^{-6}$ emu/mol, for Cu8N and Cu8P, respectively. We also corrected the data for the temperature independent paramagnetism, estimated to be $60\cdot 10^{-6}$ emu/mol of Cu for both compounds.[15]

C. NMR-NQR measurements

1. ^{1}H NMR

The proton NMR data on Cu8P were obtained with both a Stelar Broadband Spinmaster and by a MID-Continent spectrometer at resonance frequencies $v=7$, 14.1, 31, 60, 62 MHz, in the temperature range 4–300 K. We measured the NMR spectra, the nuclear spin-lattice relaxation rate NSLR (R_1) and the spin-spin relaxation rate T_2^{-1}. Moreover we measured the frequency (field) dependence of the ^{1}H NSLR at room temperature in the range 7–400 MHz. The spectra were obtained by a direct Fourier Transform of the free induction decay. The T_2 measurements were performed by using the solid echo $(\pi/2)_x-(\pi/2)_y$ sequence. The NSLR measurements were done by using a $(\pi/2)_n-\pi/2-\pi/2$ sequence where $(\pi/2)_n$ is a saturation comb of $n=1-10$ pulses, where the exact number of pulses was chosen in order to obtain the best saturation and it varies depending on the temperature and the resonance frequency of the experiment.

The recovery laws for the transverse proton magnetization are exponential at all the temperatures and frequencies investigated, yielding a well defined T_2 value. At temperatures $T>200$ K, the recovery laws of the longitudinal magnetization are also exponential yielding a single T_1 value, contrary to the lower T region ($T<200$ K) where the recovery law is nonexponential [see Fig. 1(a)]. The nonexponentiality can be ascribed to the lack of a common spin temperature among the 37 non-equivalent protons during the relaxation process. Whenever the recovery was nonexponential we measured the tangent at the origin of the recovery law which gives an average NSLR, i.e., $R_1=\Sigma_1 p_i T_{1i}^{-1}$ where T_{1i}^{-1} is the NSLR of the i-th proton or group of protons and p_i is the corresponding statistical weight.[16]

2. ^{63,65}Cu NMR

The ^{63}Cu NMR spectra, T_2 and NSLR data were collected on Cu8P with a Mid-Continent pulsed NMR FFT spectrometer in the temperature range 4.2–80 K at $H=4.7$,8.2 T. The NMR signal is lost for $T>80$ K, due to the very short T_2

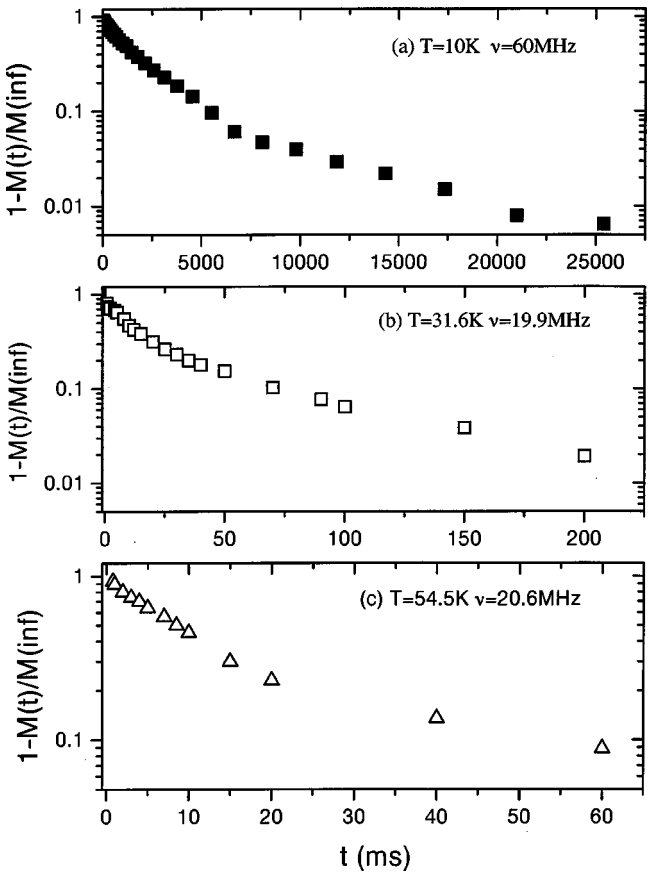

FIG. 1. Examples of semilog plots of the recovery of the longitudinal nuclear magnetization vs time: (a) proton NMR signal in Cu8P; (b) ^{63}Cu NQR signal in Cu8N; (c) ^{63}Cu NQR signal in Cu8N.

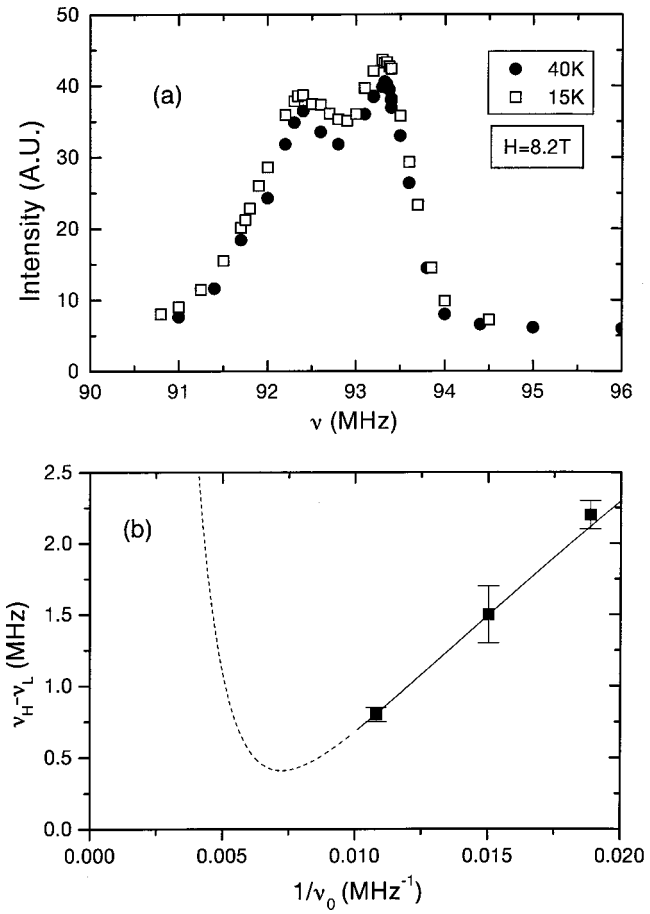

FIG. 2. (a) ^{63}Cu NMR spectra in Cu8P compound at high field, $H=8.2$ T. The two singularities typical of a NMR spectrum with second-order quadrupole interactions are well resolved in the lower T spectra. (b) The separation between the two singularities shown in part (a) of the figure, i.e., $\nu_H-\nu_L$, is plotted as a function of $1/\nu_0$ where ν_0 is the Larmor resonance frequency. The full line corresponds to the region where the quadrupole interaction is dominant. The dashed line is an extrapolation with arbitrary values of the magnetic shift parameters, which show the qualitative behavior expected at high magnetic field.

value. The spectra were mapped by plotting the solid echo amplitude as a function of the transmitter frequencies since the spectral frequency width of the irradiating radio frequency pulse is much narrower than the total NMR line width. Typical $\pi/2$ pulse length ranged from 4.5 to 7 μs depending on the experimental conditions (temperature, attenuation of RF power, etc). The measured spectra showed essentially the same features at 4.7 and 8.2 T.

^{63}Cu NMR T_2 was measured with a $\pi/2-\pi$ sequence. The recovery of the transverse nuclear magnetization could be fitted by the sum of an exponential function plus a gaussian component whereby the latter becomes comparable to the exponential component below 50 K. The temperature dependence of the transverse relaxation rate measured at different points in the spectrum was found to be different. Thus the relative intensity of the spectra at different temperature [see Fig. 2(a)] cannot be compared without proper normalization.

The NSLR of ^{63}Cu NMR were measured at the high-frequency maximum of the spectrum with a $(\pi/2)_n-\pi/2-\pi/2$ saturating sequence. The recovery curves of the longitudinal magnetization could always be fitted by a stretched exponential function, $A\cdot\exp[-(t/T_1)^{\beta}]$, with temperature-independent $\beta=0.43$. The value of β is independent of the number of pulses in the saturation sequence, ruling out the possibility of spectral diffusion. The recovery curves were only weakly dependent on the position in the spectrum. Since the spread of the NMR spectrum [see Fig. 2(a)] is mainly due to the powder pattern in presence of second-order quadrupole interactions, measurements at different positions in the spectrum correspond to measurements at different angles of the external field with respect to the electric field gradient principal axis. Thus the angular dependence of the NSLR must be small consistently with a weak anisotropic hyperfine interaction (as discussed in Sec. IV). The only explanation left for the apparently stretched exponential behavior is thus the fact that the recovery curve is the superposition of four different recovery curves due to the four nonequivalent Cu sites each of which has an intrinsic nonexponential recovery since it refers to a central line $(1/2\leftrightarrow -1/2)$ transition in presence of strong quadrupole effects.[17]

3. ^{63,65}Cu NQR

The ^{63}Cu NQR spectra, T_2 and NSLR data on Cu8P and Cu8N were obtained by a BRUKER MSL200 spectrometer, in the temperature range 4–95 K. For $T>95$ K the ^{63}Cu

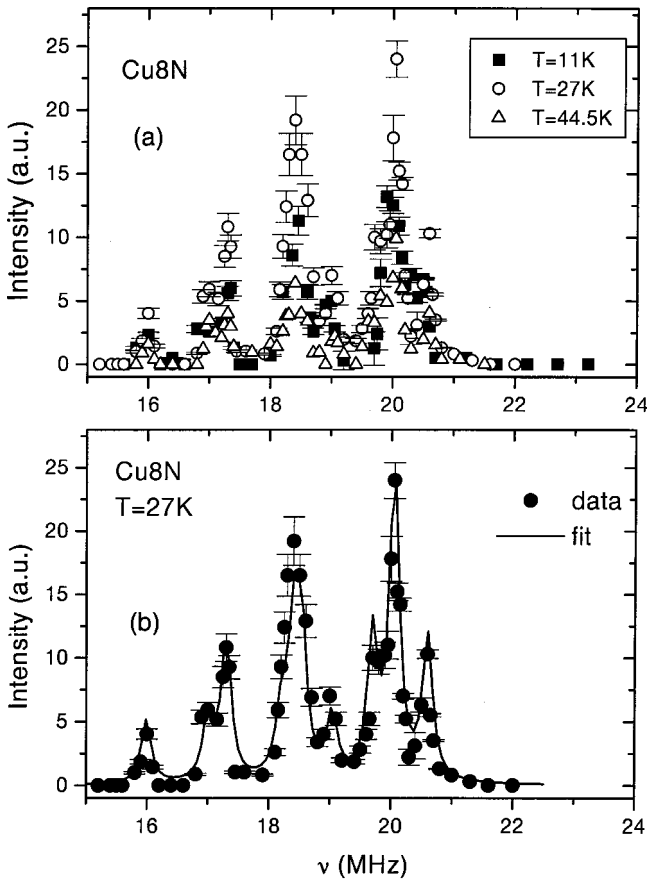

FIG. 3. (a) ^{63}Cu NQR spectra of Cu8N at two different temperatures obtained by the echo envelope technique. One can note that the shape of the spectrum remains the same at each temperature. (b) ^{63}Cu NQR spectrum of Cu8N at $T=27$ K; the solid line represents the best fit obtained by the sum of five different ''double'' lines (from ^{63}Cu and ^{65}Cu isotopes contribution). Four of these lines are due to the four nonequivalent Cu ions and the fifth one is due to the ''defects'' containing copper ions (see text).

NQR signal cannot be measured because T_2 becomes too short.

The NQR spectra, which are broader than the spectral frequency width of the irradiating radio frequency pulse, were obtained by plotting the echo amplitude as a function of the transmitter frequency.[17]

The ^{63}Cu NQR NSLR was measured by a $(\pi/2)_n-\pi/2-\pi$ saturating sequence by tuning the transmitter frequency at two different values of the resonance spectrum: $v=19.9$ and $v=20.6$ [see Fig. 3]. The recovery curve of the longitudinal magnetization is nonexponential [see Fig. 1(b) for Cu8N sample] while one would expect an exponential law for the NQR case of nuclear spin $I=3/2$.[17] We speculate that the nonexponentiality is due to the partial overlap of the different NQR lines originating from the four inequivalent Cu sites as discussed in Sec. IV.

III. MAGNETIC SUSCEPTIBILITY

The χT-vs-T curves for Cu8N and Cu8P are shown in Fig. 4. Measurements above room temperature could not be performed because the sample degrades for $T>320$ K. In

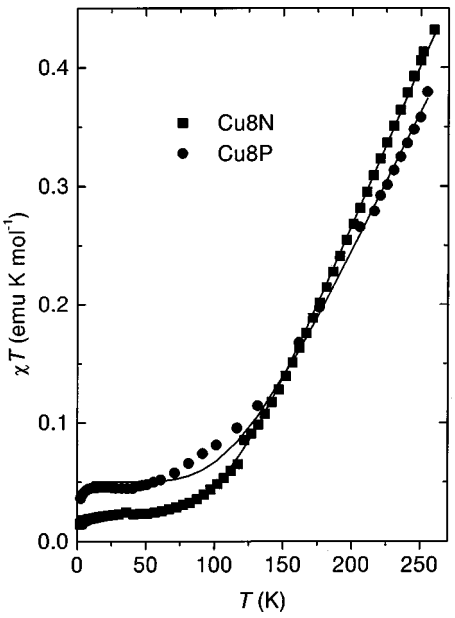

FIG. 4. Magnetic susceptibility data as a function of temperature for Cu8P and Cu8N compounds, reported as χT vs T, with $\chi=$M/H in an applied field $H=0.1$ T. The solid lines represent the best fits of the data obtained by using Eq. (1) (see text). The data plotted in figure have been already corrected for the sample holder contribution, the molecular diamagnetism and the temperature independent paramagnetism (see text).

both compounds, the value of χT at room temperature and below is very small when compared to the paramagnetic value of eight uncoupled $S=1/2$ spins (3 emu K mol^{-1} with $g=2$). This small value is by itself indicative of strong antiferromagnetic exchange interactions between the copper (II) ions, leading to a nonmagnetic $S_T=0$ ground state with a large energy gap separating it from the excited magnetic states. At low temperature the χT values do not go to zero, but level to a plateau corresponding to 0.2 emu K mol^{-1} for Cu8N and to 0.5 emu K mol^{-1} for Cu8P. This can be considered to be an evidence for the presence of paramagnetic impurities, as often observed in the magnetism of antiferromagnetic clusters. It should be remarked that the small intrinsic paramagnetic susceptibility combined with a relatively large number of paramagnetic defects in the samples reduces drastically the precision of the data which follow. In order to analyze the experimental data one has first to calculate the magnetic energy levels for a model Heisenberg hamiltonian $H=\Sigma_{ij}\mathbf{JS}_i\cdot\mathbf{S}_j$ in terms of the exchange coupling J. This can be done by numerical diagonalization of the $2^8\times 2^8=256\times 256$ matrix, by using the method of Irreducible Tensor Operators.[18] The energies of exchange multiplets, $E(S_i)$, obtained by assuming a unique coupling constant J along the ring, are presented in Fig. 5 where the multiplets are classified according to the total spin. It must be remarked that the exact solution of the exchange Hamiltonian for eight $S=1/2$ spins ring was published a long time ago.[2] The E/J values obtained by Orbach[19] are in agreement with our results.

Once the energy levels are known, the susceptibility data can be fit by the expression:

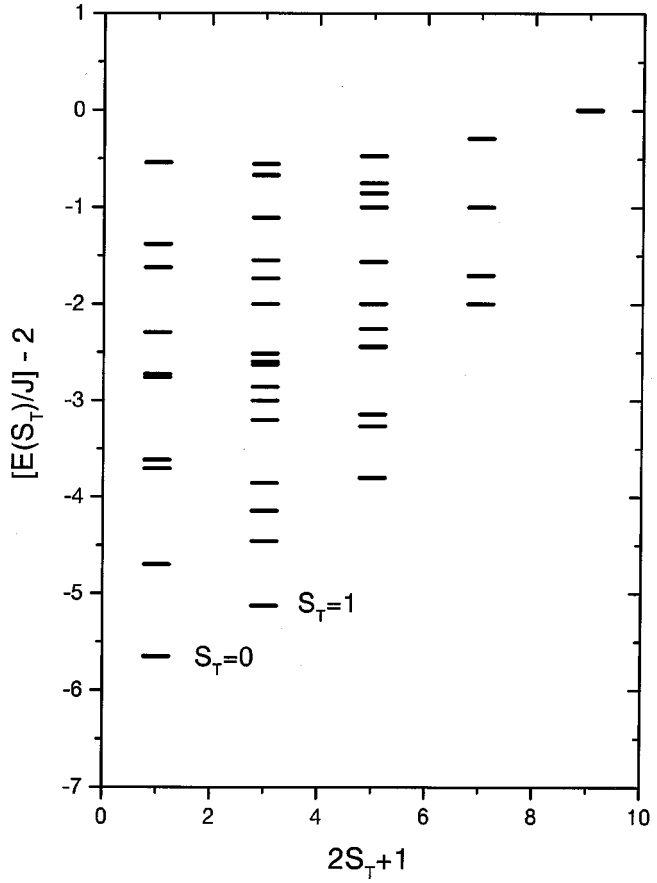

FIG. 5. Calculated theoretical values of the energy levels, reported as $[E(S_T)/J\text{-}2]$, for each $2S_T+1$ value in Cu8 where S_T is the total spin. The gap Δ between the singlet ($S_T=0$) ground state and the first triplet ($S_T=1$) excited state is $\Delta\sim 500$ K.

$$\chi T=\frac{N_A g^2 \mu_B^2}{3k_B}\times\left\{(1-\alpha)\frac{\Sigma_i S_i(S_i+1)(2S_i+1)\exp[-E(S_i)/k_BT]}{\Sigma_i(2S_i+1)\exp[-E(S_i)/k_BT]}+\alpha\frac{MW}{MW_{\rm imp}}s_{\rm imp}(s_{\rm imp}+1)\right\},\quad(1)$$

where α is the amount of impurities assumed to have spin $s_{\rm imp}=1/2$, g is the Lande' factor and μ_B is the Bohr magneton. The second term in brackets models the contribution of the paramagnetic impurities. For the sake of simplicity only one type of impurity has been considered. The g-factor and the ratio $MW/MW_{\rm imp}$ between the molecular weight of Cu8 and that of the impurity were fixed at 2.13 and 1.00, respectively, while α and J were treated as adjustable parameters. In order to minimize the uncertainties arising from the low-temperature behavior, which is dominated by the impurity contribution, we restricted our analysis to the temperature range $10<T<260$ K. The solid lines in Fig. 4 provide the best fit to the experimental data with $J/k_B=930(1)$ K and 994(4) K for Cu8N and Cu8P, respectively. The impurity content was found to be $\alpha=0.0505(13)$ and 0.118(3), respectively. Since the gap between the singlet ground state and the triplet excited state is $\Delta=0.523J$ (see Ref. 19 where J is defined as half of our J), one has $\Delta/k_B=485.9(6)$ K and 519(3) K for the two compounds, respectively. Since the measurements refer to a temperature range in which the susceptibility is small as a consequence of the large energy gap, the value of J obtained by the fit of the susceptibility may have a systematic error due to the corrections applied to the raw data and not included in the statistical error given above.

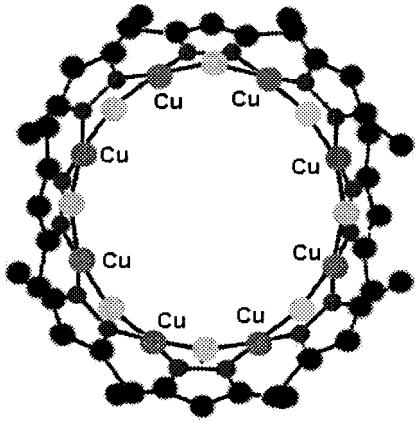

FIG. 6. A schematic molecular structure of Cu8 compound. The ring arrangement is clearly noted. The gray circles are Cu ions, the light gray O ions, the dark gray are N atoms and the black ones are C atoms. The hydrogens are not shown for clarity.

IV. NMR AND NQR SPECTRA

A. Proton NMR

The structure of the Cu8 molecular ring in Cu8N is shown in Fig. 6.[6,13] Thirty-two nonequivalent hydrogen atoms, not shown in the figure, are attached to the oxygen and carbon atoms of the octacopper (II) ring. The resulting proton NMR line is a single symmetric line, which consists of the superposition of the NMR signal from the total 37 nonequivalent protons. The line width is independent of the applied magnetic field indicating the absence of any magnetic inhomogeneous broadening. On the other hand a measurable temperature dependence can be observed in the range 300–100 K (see Fig. 7). The low-temperature limit of the linewidth (i.e., $\sim$40 KHz) can be ascribed entirely to nuclear dipole-dipole interaction among protons in the molecule. The partial line narrowing from 40 KHz down to 10 KHz on increasing T is likely to be due to the onset of molecular reorientational motion of the proton groups when the correlation times become faster than the inverse of the dipolar linewidth, i.e., $\tau\sim 2.5\times 10^{-5}$ sec.

B. ^{63}Cu NMR and NQR

The ^{63}Cu and ^{65}Cu NQR signals were detected in zero external magnetic field in one of the two samples (i.e., Cu8N). The spectra recorded at different temperatures show no significant difference [see Fig. 3(a)]. Since both ^{63}Cu and ^{65}Cu isotopes have $I=3/2$, only two NQR lines should be present with intensity ratio $I(^{63}\text{Cu})/I(^{65}\text{Cu})=2.235$ and resonance frequency ratio $\upsilon(^{63}\text{Cu})/\upsilon(^{65}\text{Cu})=1.082$. The complexity of the NQR spectrum observed in our sample indicates the presence of more than one Cu site in structurally inequivalent positions. From the inspection of the crystal structure[6] (see Fig. 6) one can distinguish four different Cu

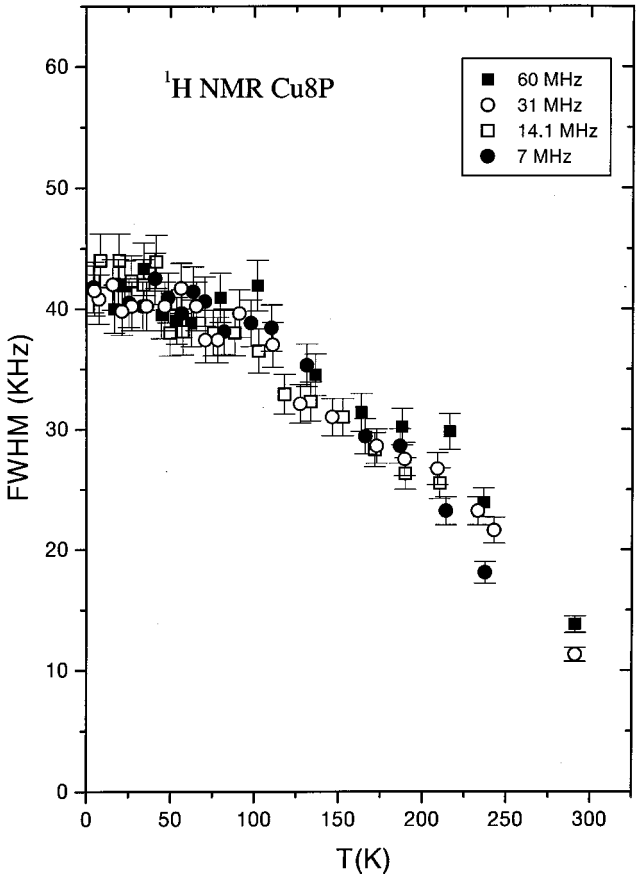

FIG. 7. Full width at half maximum (FWHM) of the ^{1}H NMR spectra of Cu8P as a function of the temperature at different frequencies of investigation.

sites in the molecule with slightly different local environment. However, four different NQR lines are not sufficient to fit the observed spectrum. It is necessary to introduce at least a fifth component in the fit. The best fit obtained using five NQR lines for each isotope is shown in Fig. 3(b). The lines are assumed to have Lorentzian shape all with the same full width at half maximum (FWHM), i.e., $\Delta\nu \approx 0.24$ MHz. The intensities of four peaks are essentially the same while the fifth peak is higher. The NQR resonance frequencies obtained from the fit are summarized in Table I. The origin of the fifth NQR signal is not presently understood. If we assume that the four equal peaks correspond to the four crystallographically different sites, then the fifth peak must correspond to undesired compounds. We explored the possibility that a sizeable amount of the precursor remains in the final powder samples. However, no NQR signal was observable in large amounts of $[Cu(dmpz)]_n$ and $Cu_8(CH_3CN)_4BP_4$ precursors in the whole frequency range 15.5–21 MHz (with particular attention to the frequency of the fifth peak at 20.05 MHz), ruling out this possibility. It is likely that the fifth NQR line arises from a large number of ''broken rings,'' some of them giving rise to paramagnetic centers, which are detected as paramagnetic impurities in susceptibility measurements. A confirmation of this scenario comes from the NQR spectra of the other sample investigated here (Cu8P). The NQR spectrum in Cu8P has broader and less-resolved NQR lines indicating a larger content of ''broken rings'' and/or other impurities, as already seen from susceptibility results.

TABLE I. Values of the quadrupole coupling frequencies ν_Q for ^{63}Cu obtained from the resonance frequencies ν_R of the NQR spectrum (Fig. 3) and using an average value $\eta = 0.1$ for the asymmetry parameter in Eq. (2).

	ν_R (MHz)	ν_Q (MHz)
Impurities	20.05	20.08
1st Cu8 peak	20.6	20.63
2nd Cu8 peak	19.7	19.73
3rd Cu8 peak	18.4	18.43
4th Cu8 peak	17.3	17.33

We turn now to the problem of determining the two components ν_Q and η of the quadrupole coupling tensor where $\nu_Q = 3e^2qQ/2hI(2I-1)$ is the quadrupole coupling frequency and $\eta = (V_{xx} - V_{yy})/V_{zz}$ is the asymmetry parameter of the electric field gradient tensor V_{ij}.[20] A NQR experiment in zero magnetic field is not sufficient to determine the two quantities separately since the resonance frequency ν_R in Table I for $I = 3/2$ is given by[20]

$$\nu_R = \nu_Q(1 + 1/3\,\eta^2)^{1/2}. \tag{2}$$

Thus measurements in an external magnetic field are necessary. The NMR spectrum in a powder sample in presence of second-order quadrupole perturbation and for $I = 3/2$ should display two singularities whose separation depends upon both ν_Q and η as follows:[21]

$$\nu_H - \nu_L = [16(1-\eta) + 8(1-\eta^2)]\frac{3\nu_Q^2}{144\nu_0} \quad (\eta > 1/3), \tag{3a}$$

$$\nu_H - \nu_L = [16(1-\eta) + (3-\eta^1)]\frac{3\nu_Q^2}{144\nu_0} \quad (\eta < 1/3), \tag{3b}$$

where ν_0 is the Larmor frequency and H,L stand for the high-frequency and low-frequency singularities respectively. Typical NMR spectra for ^{63}Cu in high magnetic field are shown in Fig. 2(a) for the Cu8P sample. One can observe the two maxima corresponding to the singularities although considerable broadening is present due partly to the effect of the impurities and partly to the presence of the four different quadrupole coupling constants (see Table I) corresponding to the nonequivalent Cu sites. The measured separation between the two singularities, i.e., $\nu_H - \nu_L$, plotted in Fig. 2(b) as a function of ν_0^{-1}, yields a slope in the low field (low ν_0) linear region of 138 MHz^{-1}. From this value and the average NQR frequency from the data in Table I and using Eq. (2) and Eq. (3b) one obtains an average $\nu_Q = 19.5$ MHz and an average $\eta = 0.1$. The small value of η is consistent with a small departure from axial simmetry of the local Cu crystal environment.[6] At high magnetic field (i.e., high ν_0) the contribution of anisotropic magnetic shift (which contains terms directly proportional to ν_0 and to ν_0^3)[21] is expected to become dominant thus making the splitting $\nu_H - \nu_L$ to turn upward for $1/\nu_0 \to 0$ (see dashed line in Fig. 2(b)). From our data one can estimate an upper limit for the isotropic mag-

netic shift ($K_{ISO} \leqslant 1\%$) and for the anisotropic magnetic shift ($K_A \leqslant 0.1\%$). With such small values, the magnetic field at which the magnetic shifts start to be detectable in the broad NMR powder spectrum is above 10 T, thus outside the reach of our experimental setup. It is noted that K_A is unusually small for the Cu-O anisotropic bond although it is consistent with the weak dependence of T_1^{-1} on the position in the spectrum (see Sec. II).

V. NUCLEAR SPIN-LATTICE RELAXATION RATE

A. Proton relaxation

The nuclear spin-lattice relaxation in Cu8 below room temperature has specific features due to the large energy gap separating the singlet ground state $S_T=0$ from the first excited state, $S_T=1$ (see Sec. III). In order to analyze the data we can refer to the theoretical expressions for the NSLR, which are commonly used in discussing the nuclear relaxation in magnetic systems.[20,22] Thus we write:

$$R_1 = \frac{\gamma^2}{2}\int_{-\infty}^{+\infty} \langle h_{\pm}(t) h_{\pm}(0)\rangle e^{i\omega_L t} dt$$

$$= \frac{\gamma^2}{2N}\sum_{\mathbf{q}} |A_{\mathbf{q}}|^2 S_{\alpha\alpha}(\mathbf{q},\omega_L), \qquad (4)$$

where we have assumed that the local transverse hyperfine field at the nuclear site is related to the local spin value, $\mathbf{S}_i$, of the Cu^{2+} magnetic ions $\mathbf{h}(t)=\Sigma_i A_i S_i(t)$. Furthermore, by introducing the $\mathbf{q}$ components of the spin variables, R_1 can be expressed in terms of the dynamical structure factor $\mathbf{S}_{\alpha\alpha}(\mathbf{q},\omega_L)$ at the Larmor frequency ω_L (with $\alpha=x,y,z$ components). We consider for simplicity isotropic spin fluctuations, i.e., $S_{xx}=S_{yy}=S_{zz}$ and $|A_q|^2$ is the form factor describing the hyperfine coupling of the spin excitations at wave vector $\mathbf{q}$ with the nuclei.

Due to the finite size of the ring the $S_T=1$ triplet excitations are characterized by only eight allowed wave vectors well separated in energy with $k=2\pi$N/8a, with N$=0,\pm1,\pm2,\pm3,4$ and $a=$Cu-Cu nearest-neighbor distance.[19] The dynamical structure factor associated to these excitations can be expressed in terms of matrix elements connecting different states with $S_T=1$:

$$S_{zz}(\mathbf{q},\omega_L) = \sum_{\mathbf{k},\mathbf{q},M_S} |\langle \mathbf{k}+\mathbf{q}, M_S | S^z_{T\mathbf{q}} | \mathbf{k}, M_S\rangle|^2$$

$$\times \delta(E_{\mathbf{k}+\mathbf{q}} - E_{\mathbf{k}} - \hbar\omega_L)\frac{e^{-E_{\mathbf{k}}/kT}}{Z}, \qquad (5)$$

where Z is the partition function and $M_S=\pm1,0$ are the magnetic quantum numbers for $S_T=1$. Since for a finite-size system the excitations are well separated in energy compared to the nuclear Zeeman energy $\hbar\omega_L$ only terms with $q=0$ and $q=2k$ satisfy energy conservation. Furthermore, at temperatures $T \ll \Delta/k_B$ where Δ is the energy separation from the $S_T=0$ ground state and the first excitations with $S_T=1$ at $q=\pi/a$ only the $\mathbf{q}=0$ are effective and one can approximate:

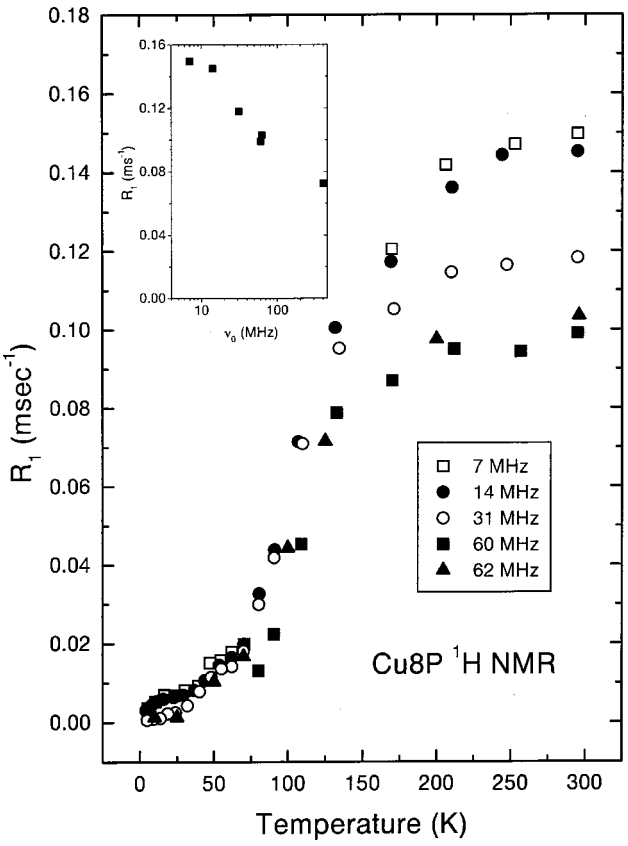

FIG. 8. Proton NMR average nuclear spin lattice relaxation rate R_1 of Cu8P as a function of temperature at different frequencies of investigation. In the inset a semilog plot of the proton relaxation rate in Cu8P as a function of resonance frequency at room temperature is shown.

$$R_1 \cong \frac{\gamma^2}{2N}|A_{\mathbf{q}=0}|^2 \frac{e^{-\Delta/k_BT}}{1+3e^{-\Delta/k_BT}}$$

$$\times \left| \left\langle k=\frac{\pi}{a}, M_S \middle| S^z_{\mathbf{q}=\mathbf{0}} \middle| k=\frac{\pi}{a}, M_S \right\rangle \right|^2 \delta(0), \qquad (6)$$

where we use the limit $\omega_L \to 0$ in the Delta function. Expression (6) can also be written in terms of the uniform susceptibility by using the fluctuation-dissipation theorem as:

$$R_1 \cong \frac{\gamma^2}{2N}|A_{\mathbf{q}=0}|^2 k_B T \chi(q=0)\,\delta(0). \qquad (7)$$

Thus one concludes that according to Eqs. (6) and (7) the NSLR should decrease exponentially at low T yielding the same gap parameter Δ as obtained from susceptibility measurements.

The proton spin-lattice relaxation rate (NSLR) measured as a function of temperature at different resonance frequencies is shown in Fig. 8. The strong magnetic field (i.e., resonance frequency) dependence at room temperature, which persists down to 100 K and below is difficult to explain. In a previous report[23] we have ascribed the room temperature field dependence (see inset in Fig. 8) to the slow decay at long time of the Cu spin autocorrelation function due to the isotropic Heisenberg interaction in a finite size system with weak correlations.

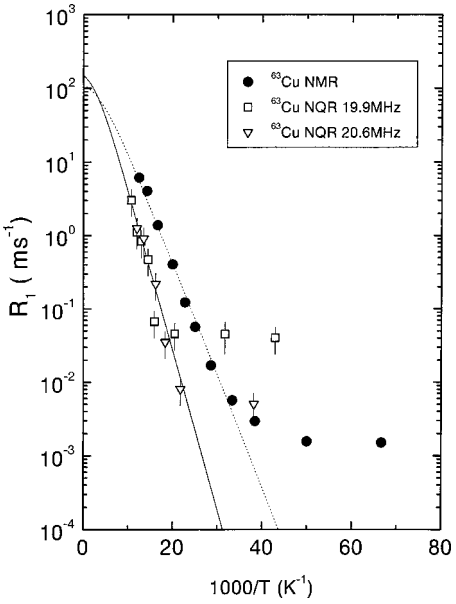

FIG. 9. Average nuclear spin-lattice relaxation rate R_1 as a function of $1000/T$, for both the ^{63}Cu NMR and the ^{63}Cu NQR. The NMR NSLR data were taken in an external field $H=8.2$ T at one of the two peaks in the spectrum ($\nu_L=93.375$ MHz). The NQR data were taken by irradiating the spectrum (Fig. 3) at two different resonance frequencies. The full line corresponds to the fitting equation $1/T_1=A\exp(-\Delta/k_BT)/[1+3\exp(-\Delta/k_BT)]$ with $A=0.6\,\mathrm{sec}^{-1}$ and $\Delta/k_B=500$ K for NQR, dotted line with $A=0.45\,\mathrm{sec}^{-1}$ and $\Delta/k_B=350$ K for NMR.

Another possibility to explain the magnetic field dependence could be the presence of a sizeable contribution to the proton NSLR due to the modulation of the nuclear dipolar interaction generated by the molecular reorientation of the proton groups. The order of magnitude of such a contribution can be estimated to be $1/T_1\sim\langle|\Delta\omega|^2\rangle\tau/1+\omega_0^2\tau^2$,[20] where $\omega_0=2\pi\upsilon_0$ is the Larmor frequency and τ is the correlation time of the molecular motion. Assuming for $\langle|\Delta\omega|^2\rangle$ the square of the low-temperature linewidth (see Fig. 7), i.e., $(2\pi\cdot 40\,\mathrm{KHz})^2$ and for τ the value ω_0^{-1} for which $1/T_1$ would have a maximum, one has at $H\approx 1$ T $1/T_1\sim 100\,\mathrm{sec}^{-1}$. Although the order of magnitude is indeed comparable to the experimental NSLR (see Fig. 8) the temperature dependence does not display the well-defined maximum, which is expected when the temperature dependent correlation time τ for molecular motions reaches the condition $\omega_0\tau\sim 1$.[20] At temperatures below 200 K the NSLR decreases exponentially (see Fig. 8) as predicted by Eq. (6) although the field dependence observed in the experimental data cannot be explained by rederiving Eq. (6) or (7) in presence of a magnetic field since the latter is a negligible perturbation with respect to the large energy gap Δ. It is likely that both the contributions due to molecular motion and the one due to the magnetic interaction with Cu^{2+} spins are relevant at $T>100$ K making their independent determination uncertain.

B. ^{63}Cu relaxation

The NSLR for the ^{63}Cu nucleus are plotted in Fig. 9 as a function of temperature. The ^{63}Cu NSLR is dominated by the magnetic relaxation mechanism associated with the fluctuations of the Cu spins. The contribution due to molecular motion is completely negligible thus making the interpretation of the data less ambiguous than for the proton relaxation. Both the NMR and NQR NSLR display an almost exponential drop on increasing T over two order of magnitude or more (see Fig. 9) reflecting the condensation of the Cu spin system into its $S=0$ ground state.

The full line in Fig. 9 corresponds to the temperature behavior of R_T predicted from Eq. (6) with a gap $\Delta=500$ K. Thus the NQR relaxation data yield a value of the gap Δ in good agreement with the one derived from susceptibility data (see Sec. III). On the other hand, the NMR relaxation data yield a somewhat smaller slope, corresponding to an effective gap value of about 350 K. The origin of this discrepancy is still unclear. It is noted that Eq. (6) was derived by neglecting the possible broadening of the triplet-state excitations due to lifetime effects and/or to intermolecular interactions. By including these effects the Delta function $\delta(0)$ in Eq. (6) and (7) should be replaced by e.g., a Lorentzian function $F_L(\omega_L)$ whose width Γ could be temperature and/or field dependent. Finally, at very low temperatures the NMR relaxation data seem to level-off to a T-independent value. This could be simply the effect of the presence of ''impurities'' in the sample which give a T-independent background nuclear relaxation.

VI. SUMMARY AND CONCLUSIONS

Two slightly different species of the octanuclear Cu(II) $S=1/2$ ring Cu8 have been characterized. The susceptibility data are consistent with a model of Heisenberg spins coupled by nearest-neighbor exchange interaction. The value of $J=950\pm 50$ K is the same for both type of rings within experimental uncertainty and the ground state is a singlet with total spin $S_T=0$ separated from the triplet excited state by a gap $\Delta/k_B=0.523\ J\approx 500$ K. The exchange interaction is likely to be dominated by the hydroxo bridge, although coupling constants in pyrazolato-bridged dicopper(II) units can reach up to 350 K.[24] In particular, the magnitude of J in Cu8 is close to that observed in copper(II) dimer containing a phtalazine- and a hydroxo-bridge with a similar Cu-O-Cu angle ($\sim 115°$).[25]

It is interesting to compare the value of the constant J obtained for Cu8 with those of other systems where two Cu ions are linked by bridges containing oxygen atoms. The data are reported in Table II. In all the copper-oxide compounds (CuO, spin ladders, high-T_c superconductors) the Cu ions are linked by an oxygen bridge (oxo bridge) and the AF exchange constant J increases by increasing the angle θ, Cu-O-Cu. In the Cu8 spin ring investigated here, the large value of J for the relatively small angle of the Cu-O-Cu bond does not correlate well with the above copper-oxide systems. Also the weak anisotropic shift, K_A, discussed in Sec. IV, which indicates a nearly isotropic magnetic hyperfine coupling tensor is at odd with the large anisotropy of the on-site hyperfine interaction in high-T_c superconductors. This is not unexpected, since it is known that the superexchange mechanism and the hyperfine interaction depend on fine features of the relative orientation of the magnetic orbitals.[26] The present results show how molecular compounds can be

TABLE II. Values of the antiferromagnetic exchange coupling constant J/k_B for an Hamiltonian $H=\Sigma_{i>j}JS_i\cdot S_J$ in copper oxides and Cu8 originating from Cu-Cu interactions. These interactions occur via different bridges characterized by the Cu-O-Cu angles reported.

Compound	Cu-O-Cu angle (degrees)	exchange constant J/k_B (kelvin)
CuO	145°	460
$Sr_2CuO_2Cl_2$	180°	1500
$Sr_{14}Cu_{24}O_{41}$ (CuI)	94°	120
$CuGeO_3$	100°	100
Sr_2CuO_3	180°	2200
La_2CuO_4	180°	1500
$YBa_2Cu_5O_6$	180°	1500
Cu8	114°7	1000

used to model the strong exchange interactions observed in inorganic materials.

The value of the gap $\Delta=500$ K found from susceptibility data is also obtained from the ^{63}Cu NSLR in the NQR (zero-field) regime. On the other hand both ^{63}Cu and ^{1}H NMR measurements in an external field seem to yield smaller values of the gap. A similar situation is found in gapped one-dimensional AF chains and ladders[27] although one can hardly invoke the same explanation in the present finite size ring. From the ^{63}Cu NQR spectrum we found confirmation for the presence of four structurally nonequivalent Cu ions with slightly nonaxial local symmetry as indicated by the small but nonzero value of the asymmetry parameter η of the nuclear quadrupole coupling tensor. The quadrupole coupling constant ν_Q is found to be around 20 MHz, a value consistent with what is found in many Cu oxide magnetic systems[11] indicating that the dominant source of electric field gradient originates from the Cu-O covalent bond.

ACKNOWLEDGMENTS

The authors thank J. E. Ostenson of the Ames Laboratory, Iowa State University, for the SQUID measurements and D. C. Johnston, M. Luban, and A. Rigamonti for useful discussions. This work was supported by the Ministero per l'Universita' e la Ricerca Scientifica e Tecnologica and Consiglio Nazionale delle Ricerche. Ames Laboratory is operated for U.S. Department of Energy by Iowa State University under Contract No. W-7405-Eng-82. This work at Ames Laboratory was supported by the Director for Energy Research, Office of Basic Energy Sciences.

[1] D. Gatteschi, A. Caneschi, L. Pardi, and R. Sessoli, Science **265**, 1054 (1994).
[2] Exact diagonalization of an Heisenberg spin ring with $S=1/2$ dates as far back as 1936: L. Hulthen, Proc. R. Acad. Sci. Amsterdam **39**, 190 (1936); see also Ark. Mat., Astron. Fys. **26A**, 1 (1939).
[3] K. L. Taft, C. D. Delfs, G. C. Papefthymiou, S. Foner, D. Gatteschi, and S. J. Lippard, J. Am. Chem. Soc. **116**, 823 (1994).
[4] A. Caneschi, A. Cornia, A. C. Fabretti, S. Foner, D. Gatteschi, R. Grandi, and L. Schenetti, Chem.-Eur. J. **2**, 1379 (1996).
[5] D. Gatteschi, A. Caneschi, R. Sessoli, and A. Cornia, Chem. Soc. Rev. **1**, 101 (1996).
[6] G. A. Ardizzoia, M. A. Angaroni, G. La Monica, F. Cariati, M. Moret, and N. Masciocchi, J. Chem. Soc. Chem. Commun. **15**, 1021 (1990).
[7] E. Rentschler, D. Gatteschi, A. Cornia, A. C. Fabretti, A.-L. Barra, O. I. Shchegolikhina, and A. A. Zhdanov, Inorg. Chem. **35**, 4427 (1996).
[8] Q. Chen, S. Liu, and J. Zubieta, Inorg. Chem. **28**, 4434 (1989).
[9] G. L. Abbati, A. Cornia, A. C. Fabretti, A. Caneschi, and D. Gatteschi, Inorg. Chem. **37**, 1430 (1998).
[10] O. Kahn, *Molecular Magnetism* (VCH, Berlin, 1993).
[11] See for example T. Shimizu, H. Yasuoka, T. Tsuda, K. Koga, and Y. Ueda, Bull. Magn. Reson. **12**, 39 (1990).
[12] G. A. Ardizzoia, G. La Monica, M. A. Angorani, and F. Cariati, Inorg. Chim. Acta **158**, 159 (1989).
[13] G. A. Ardizzoia, M. A. Angaroni, G. La Monica, F. Cariati, S. Cenini, M. Moret, and N. Masciocchi, Inorg. Chem. **30**, 4347 (1991).
[14] C. J. O'Connor, Prog. Inorg. Chem. **30**, 203 (1982).
[15] V. H. Crawford, H. W. Richardson, J. R. Wasson, D. J. Hodgson, and W. E. Hatfield, Inorg. Chem. **15**, 2107 (1976).
[16] A. Lascialfari, D. Gatteschi, F. Borsa, and A. Cornia, Phys. Rev. B **55**, 14 341 (1997).
[17] E. Fukushima and S. B. W. Roeder, in *Experimental Pulse NMR* (Addison Wesley, Reading, MA, 1981).
[18] L. Pardi and D. Gatteschi, Gazz. Chim. Ital. **123**, 231 (1993).
[19] R. Orbach, Phys. Rev. **115**, 1181 (1959); see also L. F. Mattheiss, *ibid.* **123**, 1209 (1961).
[20] A. Abragam, *Principles of Nuclear Magnetism* (Clarendon, Oxford, 1961).
[21] P. C. Taylor, J. F. Baugher, and H. M. Kriz, Chem. Rev. **75**, 203 (1975).
[22] A. Rigamonti, F. Borsa, and P. Carretta, Rep. Prog. Phys. **61**, 1367 (1998).
[23] A. Lascialfari, Z. H. Jang, F. Borsa, D. Gatteschi, and A. Cornia, J. Appl. Phys. **83**, 6946 (1998).
[24] D. Ajò, A. Bencini, and F. Mani, Inorg. Chem. **27**, 2437 (1988).
[25] L. K. Thompson, A. W. Hanson, and B. S. Ramaswamy, Inorg. Chem. **23**, 2459 (1984).
[26] *Magneto-structural Correlations in Exchange Coupled Systems*, edited by K. D. Willett, D. Gatteschi, and O. Kahn (Reidel, Dordrecht, 1985).
[27] See, e.g., G. Chaboussant *et al.*, Phys. Rev. Lett. **79**, 925 (1997); P. Carretta *et al.*, Phys. Rev. B **56**, 14 587 (1997); F. Tedoldi *et al.*, J. Appl. Phys. **83**, 6605 (1998).